Egypt. J. Chem. **Vol. 65,** No. 8 pp. 147 - 162 (2022)

Egyptian Journal of Chemistry

http://ejchem.journals.ekb.eg/

Synthesis, characterization, DFT, DNA binding, SOD like activity and hydroxyl free radical scavenging activity of binuclear bisthiosemicarbazide vanadyl (IV)$^{2+}$ complexes

Ola A. El-Gammal[1]*, Mohamed A.El_nawawy[2], Hosni A. Gomaa [2], Bassam M. Ismael[2]

[1] Chemistry Department, Faculty of Science, Mansoura University, Mansoura, Egypt

[2]Chemistry Department, Faculty of Science, Al-Azhar University, Nasr City-Cairo 11884, Egypt

Abstract

The reaction of two thiosemicarbazides, H_4DDET (2,2'-((9S,10S,11R,12R)-9,10-dihydro-9,10-ethanoanthracene-11,12-dicarbonyl)bis(N-ethylhydrazine-1-carbothioamide) and H_4DDPT (2,2'-(9S,10S,11R,12R)-9,10-dihydro-9,10-ethanoanthracene-11,12-dicarbonyl)bis(N-phenylhydrazine-1-carbothioamide) with vanadyl sulphate monohydrate salt resulted into two novel binuclear complexes. The structures of the ligands and metal complexes were elucidated by elemental analyses, spectral (FTIR, UV-vis., mass, ESR and XRD) and magnetic susceptibility as well as molar conductivity measurements. On the basis of the data obtained, the complexes afforded the molecular ormulae;$[(VO)_2(H_2DDET)(H_2O)_2(SO_4)].5H_2O$ and $[(VO)_2(H_4DDPT)(H_2O)_2(SO_4)_2].5H_2O$, respectively. IR data revealed that H_4DDET acts as a binegative NOS tridentate coordinating one metal ion in the enol-thiol form one side via C-O, ν(C=N*) and H_4DDPT as neutral $N_2O_2S_2$ through O atom of C=O, N atom of N^2H and S of C=S groups. The UV-vis. spectral data and magnetic moment values suggested an octahedral for both complexes. Also, ESR spectra of strongly coupled pairs showed a single broad line with non-homogeneous broadening. The data agree well with the subnormal magnetic moment values (μeff 1.00 and 1.18 B.M, respectively confirming a binuclear structure and the g value indicates an appreciable covalency which originates from the fact that thiolato sulphur binding in this complex incorporates greater covalency in the metal-ligand bonding through delocalized dπ –Pπ in plane π-bonding. Thermal gravimetric analysis (TGA) and differential thermal gravimetric analysis(DrTGA) study were carried out to examine the thermal stability and the nature of solvent molecules and the associated kinetic parameters of the degradation steps were evaluated. XRD study of $[(VO)_2(H_2DDET)(H_2O)_2(SO_4)].5H_2O$ indicated that the complex crystallized in cubic $C_{36}H_{81}AsCl_4N_{24}NiO_{24}S_4$ structure with lattice constant a= 12.3438 Å, b= 12.5011 Å, c= 24.4502 Å; α= 100.095º β= 90.307 º γ= 95.425 º and P -1 space group. Molecular modelling by DFT was done to determine the active sites of thiosemicarbazide moiety that appeared at carbonyl oxygen atoms, N of NH or S of C=S groups. Additionally, parameters like geometry, Mullikan population, Mullikan charge and HOMO-LUMO gap were evaluated. The title compounds were screened for antioxidant activity such as SOD-like activity and scavenging of hydroxyl radicals. Finally, the antibacterial activity was tested and the data revealed higher inhibition power on chelation.

Keywords*:* thiosemicarbazides, spectral, thiolato sulphur, XRD, Mullikan charge, SOD.

Introduction

There is no doubt that sulfur incorporating compounds and their metal complexes have received a significant interest in the last century. It is well documented that thiosemicarbazides are precursors to thiosemicarbazones. This was referred to the diversity of numerous heterocyclic derivatives such as thiazoles, pyrazoles, thia- diazoles, triazoles, thiadiazines, triazines, pyrimidines that can be generated from thiosemicarbazides [1]. This diversity is primarily correlated with the fact that these compounds can coordinate via aminic N1, N2 and N4 in thione form or through N1, N2 and S in thiol form of the thiosemicarbazide derivative [2]. The scientific researches concerning thiosemicarbazides have been enhanced paying attention on their applications in life, pharmacy and industry [3-5]. The biological activity of thiosemicarbazides as ligands is related to their strong ability to form chelates with the essential metal ions, in which the fungus needs in its metabolism. Also, they can exist in tautomeric thione- thiol [6-9]. They have shown antimicrobial, antifungal, antibacterial, anti-carcinogenic activities and insulin mimetic properties [10-14]. The antitumor activity

*Corresponding author e-mail: olaelgammal@yahoo.com.; (Ola A. El-Gammal).

Receive Date: 29 March 2022, Revise Date: 11 June 2022, Accept Date: 13 June 2022

DOI: 10.21608/EJCHEM.2022.130356.5746

might be because of an inhibition of DNA synthesis created by the modification in the reductive conversion of ribucleotide to deoxyribnucleotide [15]. In addition, a wide range of tridentate thiosemicarbazide metal complexes with unique biological effects have also been described in the literature among the effects of these ligands, including copper [16], platinum [17] or vanadium [18] compounds. Regarding vanadium, α (N) -pyridyl thiosemicarbazide complexes formed with oxovanadium (IV) and dioxovanadium (V) have been shown to have potent cytotoxic activity against human cancer cells [19], inhibiting apoptosis of malignant glioma cells [20], antiamebic activity [21], antitumor and antiviral activity [22] as well as the expression of the mimetic effect of insulin [23]. In addition, the insulin-enhancing properties of some V (V) O2-thiosemicarbazide complexes have been described [24].

It is well known that superoxide anion O2- is essential for the biological defense system towards the invasion of bacteria and viruses. It is also proved to be useful in the pathogenesis of many disease processes, including inflammatory damage, membrane and DNA damage, and aging [25-27]. Thus, a critical balance of enzymes defending against antioxidants like SOD enzymes is therefore required to maintain normal cell and organ function. However, the experimental use of SOD enzyme in biological systems may cause difficulties associated with the systematic infection of protein, i.e. the circulation lifetime, cell impermeability, immunogenicity, tissue targeting, antigenicity, and high costs. To circumvent such limitations, there are many attempts that carried out in developing synthetic SOD mimics that possess low molecular weight, biological stability, membrane permeability, and are nontoxic and cost-effect [28].

These facts motivated us to synthesize and characterize new two thiosemicarbazides as well as their corresponding vanadyl (II) complexes to study their antioxidant activity such as superoxide dismutase (SOD) like activity and hydroxy scavenging ability as well as the antibacterial activity.

2. Experimental

2.1. Instrumentation and materials

All chemicals used were of Aldrich or Fluka grade. C, H and N percent were determined using a Perkin-Elmer 2400 series II analyzer. The chloride and metal contents were determined according to the standard methods [29].IR spectra (4000–400cm−1) for KBr discs were recorded on a Mattson 5000 FTIR spectrophotometer. Unicam UV–Vis spectrophotometer UV2 was used for displaying the electronic spectra. Magnetic susceptibilities were measured with a Sherwood scientific magnetic susceptibility balance at 298 K. NMR spectra were measured using Varian nmr 400 (1H, 400 MHz; 13C, 101 MHz) spectrometer using CDCl3, or DMSO-d6 as a solvent and internal reference. Electrospray ionization (ESI) mass spectra were recorded on a Thermo Scientific (Rockford, IL, USA) Q Exactive (Orbitrap mass spectrometer). TGA, DTA measurements (20–800˚C) were recorded on a DTG-50 Shimadzu thermogravimetric analyzer at a heating rate of 10 °C/min and nitrogen flow rate of 15 ml/min. A powder ESR spectrum was carried out in a 2 mm quartz capillary at room temperature with a Bruker EMX spectrometer working in the X-band (9.78 GHz) with 100 kHz modulation frequency. XRD patterns were obtained using Philips X-ray diffractometer (model X'pert) with utilized monochromatic Cu Kα radiation operated at 40 kV and 30 mA and a scanning speed of 8 (deg /min) in the 2θ range 10°–80°.

2.2. Preparation of ligands

The ligands, H4DDET and H4DDPT were prepared by heating the hydrazide (9,10-dihydro-9,10-ethanoanthracene-11,12-diacidhydrazide) [30] with RSCN (R= allyl, ethyl phenyl and phenyl isothiocyanate), respectively, in a 1:2 molar ratio for 5 h under reflux. The obtained precipitates were immediately filtered off, washed many times with hot ethanol, dried in a desiccator over silica gel and checked by TLC and characterized by elemental analyses (C, H, N, S) and spectral (IR, Mass, 1H, 13CNMR and UV-vis.).

2.3. Synthesis of the complexes

An aqueous solution of VOSO4.H2O salt was added to ethanolic solution of H4DDET or H4DDPT dropwise in molar ratio 1:2 (L:M) and the mixture were refluxed for □ 5 hrs. Greyish green precipitates that formed were filtered off, washed with cold ethanol, and dried in a desiccator over silica gel. The complexes found to be hygroscopic and insoluble in common organic solvents but soluble in both dimethylformamide (DMF) and dimethylsulfoxide (DMSO) and the values of conductivity for 10-3 M

solution in DMF were <50 Ω-1.cm2.mol-1 indicating nonelectrolytic nature [31].

2.4. Biological activity

2.4.1. Superoxide dismutase (SOD)scavenging activity

This activity was tested using Bridges and Salin method [32]. The method is based upon the inhibitory action of SOD on the reduction of nitroblue tetrazolium (NBT) by the superoxide anion produced by the xanthine / xanthine oxidase system. The solutions of the free thiosemicarbazides as well as their corresponding VO2+ complexes were prepared in dimethylsulphoxide (DMSO). For comparative intents, the activity of L-Ascorbic acid has also been determined.

2.4.2. Antibacterial activity

The prepared compounds were tested for their antimicrobial activity by cup diffusion technique [33] against two of Gram's positive, Staphylococcus epidermidis (S. epidermidis) ATCC 12228 and Streptococcus pyogenes (Strp. py.) ATCC 19615 (Becton Dickinson Company, USA) and two Gram's negative, Escherichia coli (E. coli) ATCC11229 (Becton Dickinson Company, USA) and klebsiella spp. (kleb. spp.) 155095A (Carolina trademark, USA) bacteria. To each solution of examined compounds (mg/ml) in DMSO, 100 µl, in LBA medium (Luria-Bertani Agar) and incubated for 24 h at 30-37 ºC were added. The positive and negative controls were Ampicillin and DMSO, respectively. three times replicate for each bacterium culture and each inhibition zone was measured in mm.

2.4.3.DNA binding assay

The binding properties of the ligands and their complexes to CT-DNA have been studied using electronic absorption spectroscopy. The stock solution of CT-DNA was prepared in 5 mM Tris–HCl/50 mM NaCl buffer (pH 7.2), which a ratio of UV absorbances at 260 and 280 nm (A260/A280) of ca. 1.8–1.9, indicating that the DNA was sufficiently free of protein [34], and the concentration was determined by UV absorbance at 260 nm (ε = 6600 Mol-1cm-1). Electronic absorption spectra (200–700 nm) were carried out using 1 cm quartz cuvettes at 250C by fixing the concentration of ligand or complex while gradually increasing the concentration of CT-DNA (0.00–7.3x 10-6 mol L-1). An equal amount of CT-DNA was added to both the compound solutions and the references buffer solution to eliminate the absorbance of CT-DNA itself. The intrinsic binding constant Kb of the compound with CT-DNA was determined using the following Eq.(1) [34]:

$$[DNA]/(\varepsilon_a-\varepsilon_f)=[DNA]/(\varepsilon_a-\varepsilon_f)+1/K_b\,(\varepsilon_a-\varepsilon_f) \quad (1)$$

Where [DNA] is the concentration of CT-DNA in base pairs, εa is the extinction coefficient observed for the Aobs/[compound] at the given DNA concentration, εf is the extinction coefficient of the free compound in solution and Kb is the extinction coefficient of the compound when fully bond to DNA. In plots of [DNA]/(εa - εf) versus [DNA], Kb is given by the ratio of the slope to the intercept.

2.5. Molecular modeling

DMOL3 module calculations were used to examine the cluster estimations [35] and double numerical basis sets plus polarization functional (DNP) implemented in Materials Studio bundle [36]. It is designed for the realization of large-scale density functional theory (DFT) calculations [37]. The geometric optimization is performed without any symmetry restriction.

3. Results and discussion

3.1. General characterization

The most important assignment of IR spectral bands of investigated thiosemicarbazides; H4DDET and H4DDPT and their vanadyl corresponding complexes (as KBr discs) were studied by careful comparison with the spectrum of the starting hydrazide, namely 9,10-dihydro-9,10-ethanoanthracene-11,12-dihydrazide and are represented in table 2 and figures 1A-1D. The data indicated the possibility of coordination of the ligands in Keto/thione or enol/thiol.

IR spectra of the thiosemicarbazides (Structures a & c) show three bands at 3271, 3218, 3189 and 3060 cm-1 assignable to ν(N4H), (N1H), ν(N2H) and aromatic CH modes, respectively. These bands appeared as broad ones in the IR spectra of metal complexes may be arising from an overlap of the stretching vibrations of lattice water molecules with the ν(NH)'s as shown in picture 1 [38].The carbonyl bands are observed as doublet at (1710 , 1711 cm-1) and (1680, 1684 cm-1) due to ν(CO) (free) and hydrogen bonded ν(CO) modes [38]. The appearance of ν(NIH) at lower wavenumber in addition to weak bands at 1900-2100 and 2300-2500 cm-1 regions

confirm the presence of intramolecular hydrogen bonding N-H-O [39].

The medium bands located at (1518-1561), (1291-1301), (917, 920) and (790-799) cm-1 in the spectra of both thiosemicarbazide derivatives may be assigned to thioamides I-IV have substantial contributions from ν(C=N), δ(C-H) and δ(N-H) [38].Also, the band due to ν(N-N) is observed at 1023 and 1010 cm^{-1}.

In the IR spectrum of H4DDET (Structure a) the doublets at 2931 and 2971 cm-1 are attributed to symmetric and asymmetric stretching vibrations of -CH2-CH3 and CH groups while the band due to ν(C=C)phenyl appeared at 1596 cm-1. The possibility of thione /thiol tautomerism in the solid state is ruled out, since no characteristic bands for thiol group (2500-2650 cm-1) are observed in the spectrum of the ligand [39].
In $[VO)_2(H_4DDET)(H_2O)_2(SO_4)].5H_2O$ complex (Structure b) , the ligand acts as a binegative NOS tridentate coordinating one metal ion in the enol-thiol form one side via C-O, ν(C=N*) and C-S and the other metal ion in keto-thione via C=O and N2H and C=S groups from the other side. This behavior is confirmed by the weakness of bands due to ν(C=O), ν(N1H), ν(C=S) and ν(N2H) modes with appearance of bands at 1561, 1132 and 615 cm-1due to ν (N=C)*, (C-O) and ν(C-S) suggesting the possibility of enolization-thioenolization of C=O and C=S groups in this thiosemicarbazide arm followed by loss of two protons on coordinating one oxovanadyl (IV) ion. The spectrum of binuclear $[(VO)_2(H_4DDPT)(H_2O)_2(SO_4)_2].5H_2O$ complex (Structure d), H_4DDPT as neutral $N_2O_2S_2$ through O atom of C=O, N atom of N_2H and S of C=S groups as confirmed by shift bands attributed to these groups to lower wavenumber. Some useful notifications can be drawn:

The shift of ν(N-N) band to higher frequency which may be referred to the increase in the band strength as a result of the participation of azomethine group in the coordination with the metals [40].

The bands that located at 1211, 1050, 980 and 453 cm-1 are due to ν3, ν1, ν4 and ν2 of the sulphate ion suggesting its bidentate nature [41].

The new band at (535, 458 or 544 cm^{-1}) assigned to ν(V-O) is evidence of chelation through C=O [41].

Also, the band at 994 or 992 cm-1assignable to ν(V=O) which overlapped with ν2 band of SO4-2 group.

3.2. NMR spectra

The 1H NMR spectrum displayed in d6-DMSO of H4DDPT ligand as a representative example is shown in figures 1a-1c and the data in table 4 that indicates three broad singlet signals at δH (ppm): {10.04, 10.26 ppm); (9.08, 9.28) and (7.63, 7.47) referring to the N1H, N2H and N4H protons, respectively. These signals disappeared upon adding D2O suggesting that they are easily exchangeable and suffer shift to downfield as they are easily subjected to hydrogen bonding with CO or CS. The protons of each N4H appear singlet as expected since the NH protons are decoupled from the nitrogen atoms and the protons from the adjacent atoms. The condensed aromatic regions revealed the presence of 18 protons which were observed as multiplets at δH (ppm):{(6.98-7.35); (7.00-7.40), (6.99-7.45)}, respectively for the thiosemicarbazides The protons of CH groups in H4DDET (CH13-CH14) (Scheme1) appear at δH 3.53 (brs, 2H) and (CH15-CH19) at 4.87 ppm (brs, 2H). The configuration of the only two sterogenic centers C15 and C19 occurred as 15S and 19S as a result of the appearance of two broad singlets for H15 and H19 instead of two doublets. The two multiplet signals observed at δH 4.02 and 4.20 ppm are assignable to the protons of two aliphatic CH2 groups. Finally, the absence of SH signal confirmed that the ligand is in the thione-keto form in the solution[41].
On the other hand, 1HNMR study was further carried out for H2DDPT. CH groups (CH13-CH14) (Structures a & c) appear at δH 3.28 (brs, 2H) and (CH15-CH19) at 4.88 ppm (brs, 2H). The configuration of the only two sterogenic centers C15 and C19 occurred as 15S and 19S as a result of the appearance of two broad singlets for H15 and H19 instead of two doublets. The two multiplet signals observed at δH 4.02 and 4.20 ppm are assignable to the protons of two aliphatic CH2 groups. Moreover, the signal centered at δH 5.82 ppm (m, 1H) is assigned to the proton of the allyl group (CH-29). Finally, the absence of SH signal confirmed that the ligand is in the thione-keto form in the solution[41].

The 13C NMR (Fig.2a) spectra of H4DDET revealed the existence of 24 carbon atoms including two methyl groups at δc 14.5 ppm, two methylene groups at 38.5, four aliphatic methine groups at 45.3 and 46.6, two amidic carbon atoms at 171.6, two

thione groups at 181.4 and eight aromatic methine groups from 123.2 to 143.0 ppm. Also, the aliphatic (CH) groups correlated to aromatic carbon atoms. On other hand, the aliphatic protons at δH 3.28 ppm attached to the amidic carbon atoms at δc 171.6 ppm.

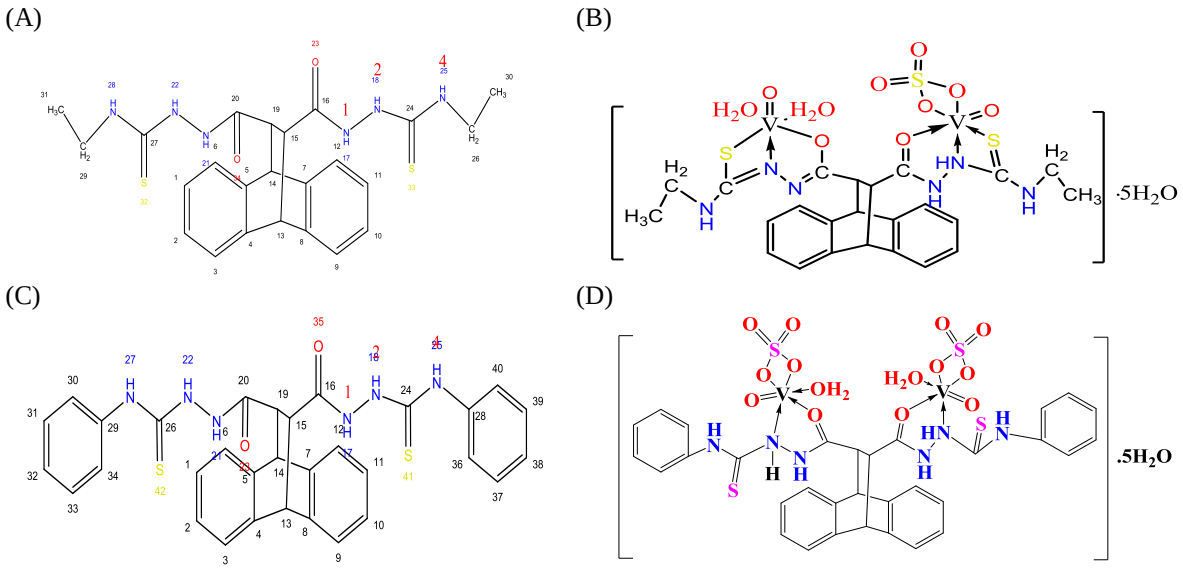

Scheme1: Structures of thiosemicarbazides and their VO^{2+} complexes

On the other hand, the 13C NMR, DEPT (fig.2a, 2b) and HSQC spectra of H4DDPT (Fig. 2c) of H4DDPT confirmed the existence of 32 carbon atoms including 4 CH aliphatic, 18 CH aromatic and 10 quaternary carbon atoms. Also, the HMBC spectrum of H4DDPT (Fig. 2d) indicated the correlation between the aliphatic (CH) groups that observed at 31.4 and 45.3 ppm with the two amidic carbonyl groups (C14, C15)} that appeared at δ: 171.2 and 169.0 ppm. The other two aliphatic CH groups, that are correlated with the other two aliphatic CH groups of the two phenyl moieties at δ: 168.0 ppm. The signal observed at δ: 178.4 ppm is referred to C=S group [41].

3.3. Electronic spectra

The magnetic moments and the electronic

absorption bands of H4DDET and H4DDPT in addition to their vanadyl complexes, in DMSO and Nujol mull, are given in Table 3. The spectra of the thiosemicarbazides (fig.3a & 3c) exhibited two shows two broad bands at {36495 cm-1 (274.01nm) & 33785 (295.98nm) and {(335.95, 402.01nm) arising from π→π* a combination of the transitions due to those of benzene ring, carbonyl and thione groups and those observed at 26450, 26740 cm-1(378.07, 373.97nm), presumably n→π*, a combination of the transitions due to those of carbonyl and thione groups of the title thiosemicarbazide derivatives, respectively [42-44]. On comparing with the ligand spectra. The following important points are noticed:

i. The spectra of metal complexes showed intra-ligand bands at 35971,36101 and 33500,32051 cm-1 attributed to π→π* transition of phenyl ring and carbonyl and/or thione groups, respectively. The n→π* transition bands suffer a noticeable great change upon complexation and appeared at 25188-27397 cm-1 indicating the chelation of central metal ion through the carbonyl and thione groups.

ii.The bands at {611, 544 nm (16340 and 18380cm-1) in the spectra of [(VO)2(H2DDET)(H2O)2(SO4)].5H2O complex (Fig.3b) are common to vanadyl systems in terms of Ballhausen and Gray model for the one electron transitions [45] and

attributed to 2B2 2E (v1) and 2B2g 2B1(v2) transitions consistent with a distorted octahedral structure [45]. Also, the dark green color may be considered as additional evidence such postulation.

iii. The electronic spectrum of [(VO)2(H4DDPT)(H2O)2(SO4)2].5H2O (Fig.3d) shows bands at {505nm (198011 cm-1) and 556 nm (17985 cm-1) assigned to 2B2 2E(v1) and 2B2g 2B1(v2) transitions in agreement with a distorted octahedral structure for oxovanadium(IV)[108].Also, the color (dark green) may be considered as further evidence for such postulation [46].

iv. The magnetic moment values of the binuclear complexes per one atom are found to be 1.00 and 1.18 B.M, respectively that are low and are in accordance with binuclear complexes having magnetic exchange interaction as will be further supported by ESR.

Table 1: Analytical and physical data of thiosemicarbazides and their vanadyl complexes.

Empirical formula	F.wt. Found (Calcd)	Color	M.p. ◦c	Elemental analyses % Found (Calcd)				
				C	H	N	S	M
H_4DDET $C_{24}H_{28}O_2N_6S_2$	496.00* (496.65)	White	260	55.62 (55.62)	5.49 (5.42)	16.90 (16.92)	12.86 (12.91)	-
$[(VO)_2(H_4DDET)(H_2O)_2(SO_4)].5H_2O$ $(VO)_2C_{24}H_{27}O_{11}N_6S_4$	806.23* (805.63)	Green	>300	33.85 (33.89)	4.09 (4.74)	10.13 (10.42)	15.67 (15.92)	12.90 (12.65)
H_4DDPT $C_{32}H_{28}O_2N_6S_2$	592.00* (592.74)	white	280	64.84 (64.84)	4.19 (4.76)	14.30 (14.18)	10.70 (10.82)	-
$[(VO)_2(H_4DDPT)(H_2O)_2(SO_4)_2].5H_2O$ $V_2O_2C_{32}H_{42}O_{19}N_6S_4$	1000.13* (1044.85)	Dark green	>300	37.89 (36.78)	4.33 (4.05)	8.15 (8.04)	12.64 (12.27)	9.99 (9.75)

***: obtained by mass spectra.**

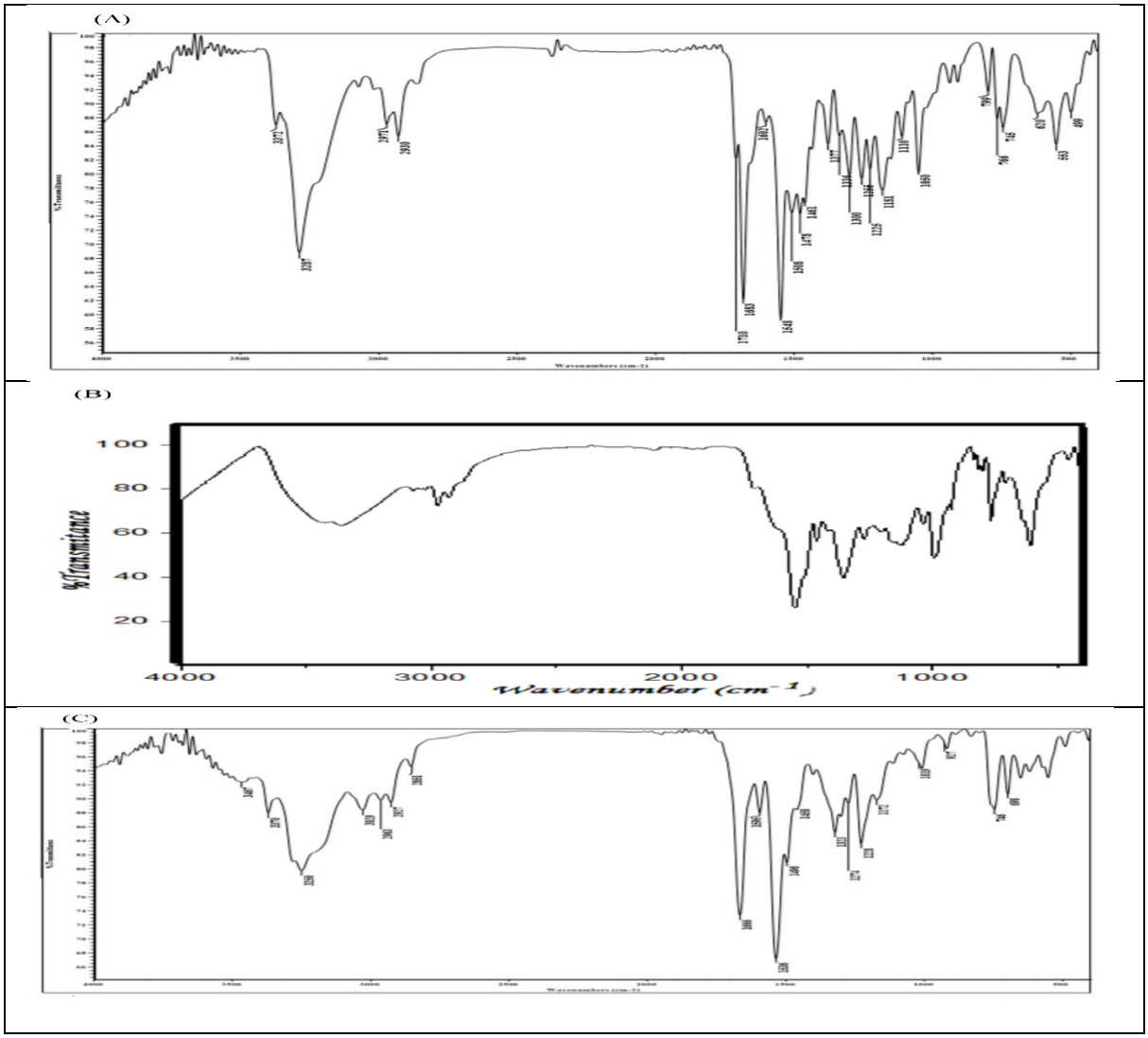

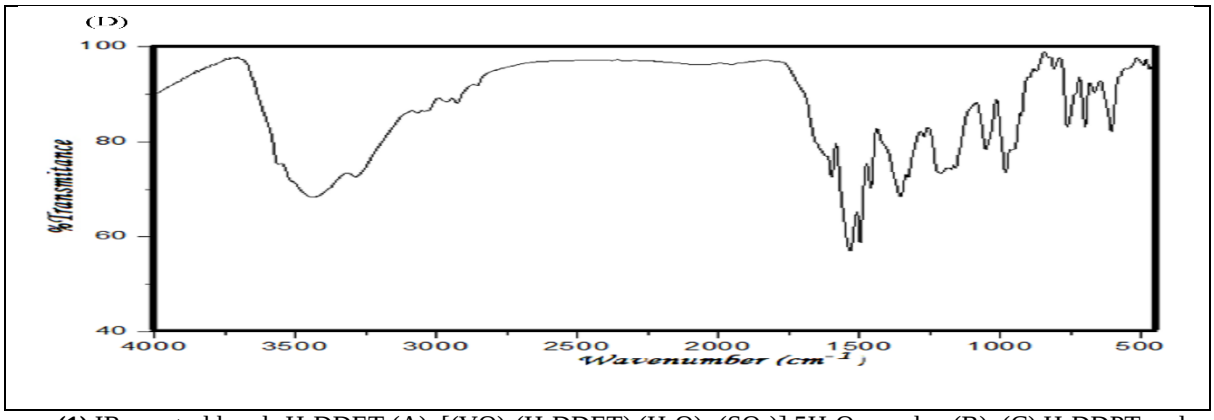

Figure (1) IR spectral bands H_4DDET (A), $[(VO)_2(H_4DDET)(H_2O)_2(SO_4)].5H_2O$complex (B), (C) H_4DDPT and $(VO)_2(H_4DDPT)(H_2O)_2(SO_4)_2].5H_2O$ complex (D)

Table 2. Assignment IR bands of thiosemicarbazides and their vanadyl complexes and their VO^{2+} complexes

.

Compound	ν(N^4H)	ν(N^2H)	ν(N^1H)	ν(N-N)	ν(C=O)	ν/δ(C=S)	ν (C=C)	ν(C=N)*	ν (C-O)
H_4DDET	3271s	3189s	3218w	1023_m	1710_m 1680s	1242s, 797s	1597_m	-	-
$[(VO)_2(H_4DDET)(H_2O)_2(SO_4)].5H_2O$	3364_m	-	-	924_m	-	799_m 739_w	1591_s	1545	-
H_4DDPT	3290_m	3249_m	3191_w	1010_m	1671_m 1665_m	1288_m 790_m	1596_m	-	-
$[(VO)_2(H_4DDPT)(H_2O)_2(SO_4)_2].5H_2O$	3286_m	-	-	1050_m	1677_w 1597_w	761_w	1597_m	1532_m	666_m

***:S=strong, w=weak, m=medium and b=broad**.

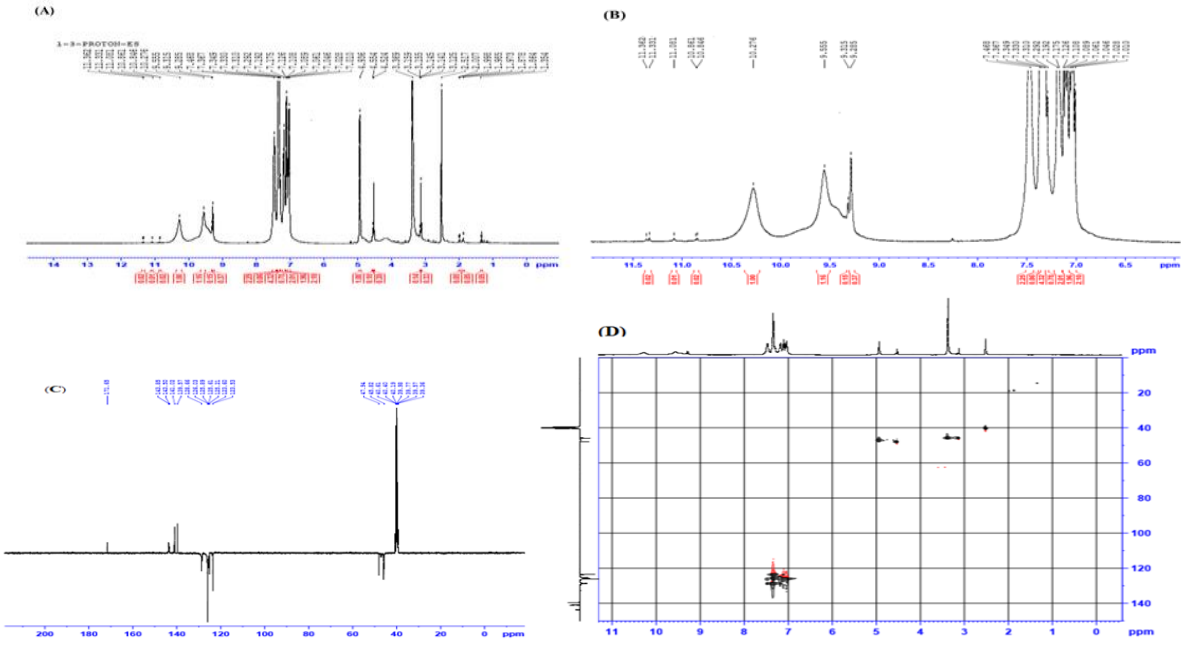

Figure 2. ^{1}NMR spectra of H_4DDPT in d_6DEMSO. ^{1}HNMR (A), ^{13}CNMR (B) and HSQ2 (C).

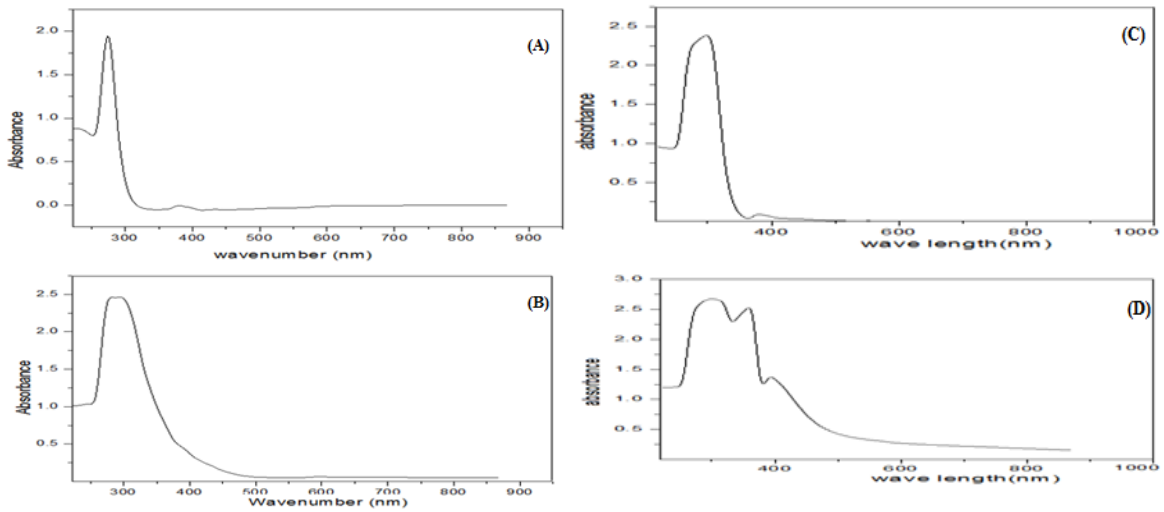

Figure 3. UV-vis. Spectra of H_4DDET (A), [$(VO)_2$(H_4DDET) (H_2O)$_2$ (SO_4)].5H_2Ocomplex (B), (C) H_4DDPT and $(VO)_2$(H_4DDPT)(H_2O)$_2$(SO_4)$_2$].5H_2O complex (D) in DMSO

Table 3. Spectral absorption bands, magnetic moments and ligand field parameters of ligands and their divalent complexes. Their divalent complexes.

Compound	Band position, cm^{-1}	μ_{eff} (B.M.)	Geometry
H_4DDET	36495, 26450	--	--
[$(VO)_2$(H_4DDET) (H_2O)$_2$ (SO_4)].5H_2O	33785,20240,22830,19920,18380,16340	1.00	Oct.
H_4DDPT	36101, 32051,27397	--	--
[$(VO)_2$(H_4DDPT)(H_2O)$_2$(SO_4)$_2$].5H_2O	32895,27930,25000	1.18	Oct.

*μ_{eff} values per one atom

Table 4. Selected ^{1}H, ^{13}C and ^{15}N chemical shifts (δ) of compounds **1–4** in DMSO-d_6.

Compound	^{1}H						^{13}C				
	N^1H	N^2H	N^4H	Cond.Ar., Side Ar.CH*	The protons of CH groups						
H_4DDET	10.04	9.08	7.63	6.98-7.35	CH13-CH14, CH15-CH19	Side Ali. CH_2	C=O	C=S	CH13-CH14, CH15-CH19	Cond.Ar., Side Ar.CH*	Side Ali. CH_2
					3.53 4.87	4.02 4.20	171.60	181.40	39.57, 45.82	123.2-143.0	45.30
H_4DDPT	10.26	9.28	7.47	7.00-7.40, 6.99-7.45	3.28 4.88	-	171.20, 169.00	178.40	14.50, 38.51 31.40, 45.32	123.50-143.80, 123.60-183.50	46.60

*Cond.=condensed; ali. = aliphatic; Ar.=aromatic; *: only in H_4DDP

3.4. ESR spectra

ESR spectra of both vanadyl complexes in the powder form was displayed at room temperature. The spectrum of both[(VO)2(H2DDET)(H2O)2(SO4)].5H2O and [(VO)2(H4DDPT)(H2O)2(SO4)2].5H2O complexes are similar (Fig. 4a & 4b) are similar to many spectra of VO2+ complexes that showed a single broad line centered at g = 1.98 without resolved hyperfine structure. The absence of vanadium hyperfine coupling is common in solid state samples and is attributed to the simultaneous flipping of neighboring electron spins or due to strong exchange interactions, which averages out the interaction with the nuclei or due to the existence of binuclear or polymeric structure [46]. Generally, the mononuclear VO2+ ion (S = 1/2, I = 7/2) has a characteristic octet ESR spectrum showing the hyperfine coupling to the 51V nuclear magnetic moment. Upon the existence of two VO2+ ions, the two electron spins may combine to a nonmagnetic spin singlet (S = 0) or a paramagnetic triplet (S = 1); only the latter is ESR detectable. The

super exchange interaction between the two vanadyl ions lead to a configuration in which the two electron spins have an antiferromagnetic character, i.e., the singlet state is energetically favored. Therefore, the ESR spectrum of strongly coupled pairs has the form of a single broad line with nonhomogeneous broadening. The data agree well with the subnormal magnetic moment values for both investigated vanadyl complexes (1.00 &1.18 BM) and confirm a binuclear structure. The index of tetrahedral distortion (f(x)=g||/A) are 164 and 184 indicating a moderate degree of distortion around the vanadium site. Also, the decrease of the g value than 2.0023 is an approximate measure of the ligand field strength; the stronger the ligand field the smaller the decrease in the g value. Also, the g value indicates an appreciable covalency which originates from that thiolato sulphur binding in this complex incorporates greater covalency in the metal-ligand bonding through delocalized dπ-ρπ in-plane π-bonding [46].

3.5. Mass spectral study

The mass spectrum of H4DDET is taken as a representative example that showed the parent peaks at m/z = 496.65 (25.93%) C24H28N6O2S2 followed by successive degradation peaks with different intensities at m/z values as illustrated in figure 5.

3.6. X Ray powder diffraction

The XRD patterns of solid powdered [(VO)2(H2DDET)(H2O)2(SO4)].5H2O and [(VO)2(H4DDPT)(H2O)2(SO4)2].5H2O are represented in figures 6 (A & B) and the data are depicted . An insight to the pattern represented in Figure 6A indicates that all of the diffraction peaks were perfectly indexed into the cubic C36H81AsCl4N24NiO24S4 structure with lattice constant a= 12.3438 Å, b= 12.5011 Å, c= 24.4502 Å; α= 100.095º β= 90.307 º γ= 95.425 º and P -1 space group. This is in good agreement with the Joint Committee for Powder Diffraction Studies (JCPDS) File No. 96-433-2969[47]. Finally, many peaks (at 2□□□11, 21, 23.5 and, 25º) and one board peak (2□□22º) are appeared in the XRD spectrum attributed to the structural nature of H4DDET ligand meaning that the free ligand of that complex presented as semi crystalline form. On the other hand, it is clear from the XRD pattern (Fig.6B) of [(VO)2(H4DDPT)(H2O)2(SO4)2].5H2O, the diffraction pattern was measured for the comlex and shows that an amorphous structure obtained for the polymerization of the free ligand [H4DDPT] at the SO4 group in vanadium metal which formed five rings in the structure matrices [47] .

3.7. TGA, DrTGA and Kinetic Study

TG curves of H4DDPT thiosemicarbazide and its [(VO)2(H4DDPT)(H2O)2(SO4)2].5H2O complex are represented (7a & 7b). The TG curve of H4DDPT (fig.7a) undergoes degradation in two steps. The first step represents the removal of (2H2O+2C6H4+2H2S) fragments (Found: 43.23%; Calcd:44.62%) at 213-2550C followed by the elimination of (2C6H5NH+2N2) moieties (Found: 40.20%; Calcd:40.53%) in the second step at 256-3340C. The residue was 8C. On the other hand, TG curve of the corresponding binuclear complex,[(VO)2(H4DDPT)(H2O)2(SO4)2].5H2O (fig.7b) exhibited the first decomposition stage at 31-110 °C attributed to loss of two water molecules (Found: 4.28%; Calcd.: 4.33%) which evidenced the presence of these molecules as water of crystallization (outside coordination sphere). The other decomposition stages of the ligand and its binuclear complex leads to residue compromise carbon ash (8C) and 8C +2VO2, respectively.

Finally, the kinetic and thermodynamic parameters for thermal degradation stages using Coats-Redfern and Horowitz-Metzger models [48, 49] have been evaluated and represented (figs.8a & 8b). The activation enthalpy (ΔH*), entropy (ΔS*) and free energy (ΔG*) were calculated by Eyring equation [49]. The activation energy, (Ea), increases or decrease for the subsequent degradation steps according to the stability of the remaining species. The positive value of ΔG*for some metal displayed that the rate of ligand removal will be lower from step to the subsequent step that may be because the oversize structural rigidity of remaining complex after the removal of one or more ligand moieties. The negative values of ΔS* indicate that the activated fragments have more ordered structure than the undecomposed fragments and the degradation reactions are slow [50].

3.8. Computational studies

3.8.1. Geometry optimization

The molecular structures along with atomic numbering of H4DDET, H4DDPT as well as their V(IV)O2+complexes are shown in (Scheme 2). The bond length and bond angle of all compounds were

listed in Tables S2-S12(supplementary material). coordination; On comparing the data of the thiosemicarbazide derivatives under investigation with corresponding complexes, it is clear that:

i. The bonds of the coordination sites are enlarged or shortened than that previously found in present ligands e.g., C-O, C-N and/or C-S as a result of M-O, M-N and/or M-S formation and there is a significant variation in N-N bond lengths of both ligands due to the coordination takes place via N-atoms of the N2H group. The following order is drawn: M-Nazomethine; V-S >V-N >V-O indicating the large strengthens of Vanadium- Oxygen donor atom rather than the others [51].

ii.The bond angles of the ligands were decreased or increased due to formation of four, five and/or six-membered chelate [51]. The largest change affects in N(18)-C(24)-N(25), C(16)-N(17)-N(18), N(19)-C(26)-N(20), C(26)-N(20)-N(21), N(18)-C(24)-S(35), N(25)-C(24)-S(35), N(19)-C(26)-S(36), N(22)-C(26)-S(36), O(23)-C(16)-N(17), O(34)-C(20)-N(21), O(34)-C(20)-C(19), (C(18)-C(16)-N(17), N(22)-N(21)-C(20) angles [54]. The bond angles of ligand moiety holding donor centers in general will be varied in all particular compounds as a result of N-M-O or N-M-S chelate ring formation are in accordance with

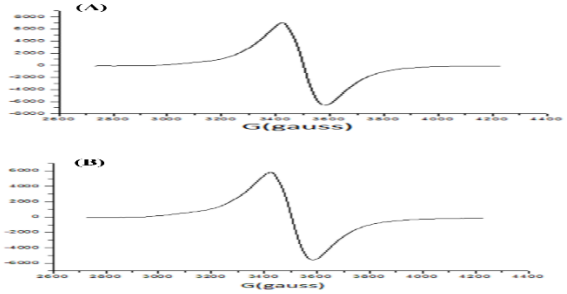

Figure 4.X-band ESR spectrum of. $[(VO)_2(H_4DDET)(H_2O)_2(SO_4)].5H_2O$ (A) and $(VO)_2(H_4DDPT)(H_2O)_2(SO_4)_2].5H_2O$ complex (B).

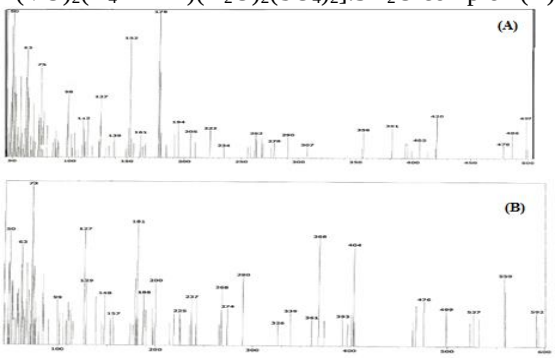

Figure 5. Mass spectra of $[(VO)_2(H_4DDET)(H_2O)_2(SO_4)].5H_2O$(A) and $[(VO)_2(H_4DDPT)(H_2O)_2(SO_4)_2].5H_2O$ (B).

distorted octahedral geometry in complexes of H4DDET and H4DDPT indicating sp3d2 hybridization [51].

3.8.2. Chemical reactivity descriptors

HOMO (π-donor) and LUMO (π-acceptor) called the frontier molecular orbitals (FMOs). The FMO's energies, EHOMO and ELUMO in addition to energy gap, ΔEH–L, shown in table 7 (Scheme 3, 4), explains the charge transfer interaction within the molecule. The chemical reactivity descriptors like chemical potential (μ), electronegativity (χ), global hardness (η), global softness (σ) and global electrophilicity index (ω) for ligands and its complexes were calculated [52]. The obtained EHOMO and ELUMO of all compounds are negative revealing their stability. The energy gap values, ΔEHOMO–LUMO of the ligands (H4DDET & H4DDPT), are -3.599, -2.903 and -3.281 eV, respectively that is an indication of higher excitation energies and therefore good stability. It is a fact that the smaller energy gap of the molecule, the more polarizable and softer it will be and the easier the ability to give electrons to an acceptor. As it depicts the toxicity estimates the stability in energy when the system gains supplemental electronic charge [53]. The ectrophilicity index (ω) is considered to be the most interesting quantum chemical descriptors.

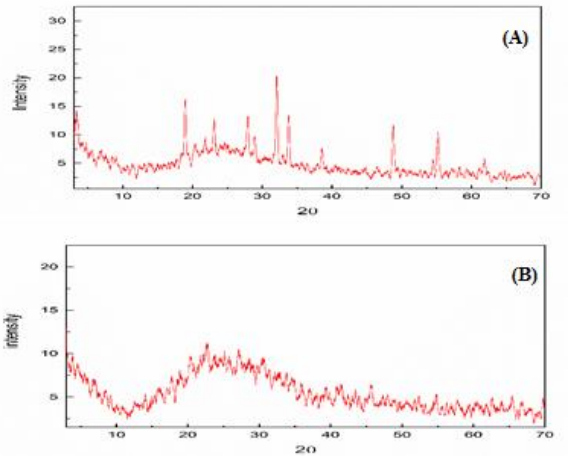

Figure 6. XRD pattern of $[(VO)_2(H_4DDET)(H_2O)_2(SO_4)].5H_2O$ (A) and $(VO)_2(H4DDPT)(H_2O)_2(SO_4)_2].5H_2O$ complex (B).

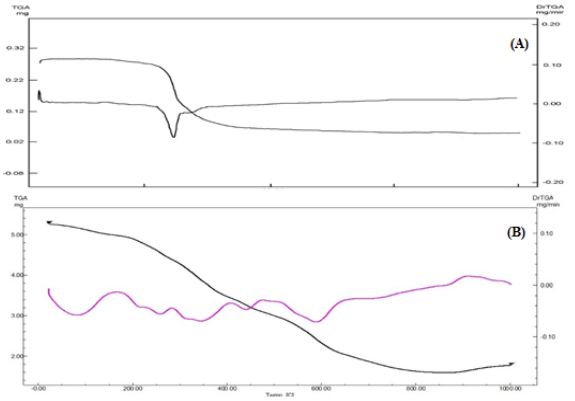

Figure 7. TGA and DrTGA curves of H_4DDPT(A) and $(VO)_2(H_4DDPT)(H_2O)_2(SO_4)_2].5H_2O$ complex (B).

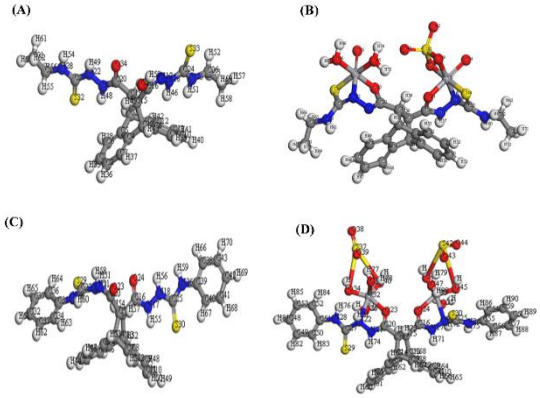

Scheme 2: Optimized molecular structure of (A)H_4DDET (B); $[(VO)_2(H_4DDET)(H_2O)_2(SO_4)].5H_2O$ (2); (C)H_4DDPT; (D) $VO)_2(H_4DDPT)(H_2O)_2(SO_4)_2].5H_2O$.

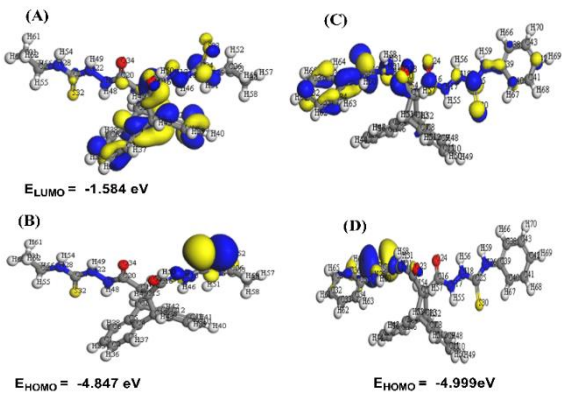

Scheme 3: HOMO and LUMO of: H_4DDET(A),(B) and H_4DDPT (C),(D).

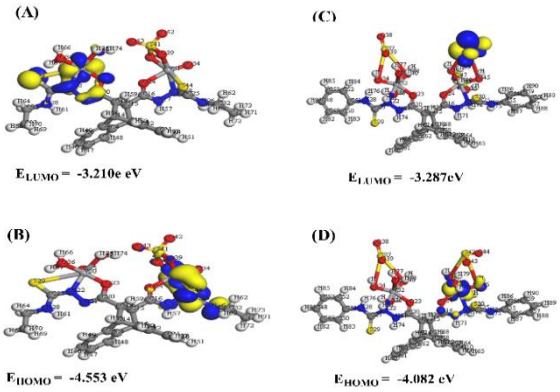

Scheme 4. HOMO and LUMO of $[(VO)_2(H_4DDET)(H_2O)_2(SO_4)].5H_2O$ (A) HOMO,(B) LUMO and $[(VO)_2(H_4DDPT)(H_2O)_2(SO_4)_2].5H_2O$. (C) HOMO, (D) LUMO

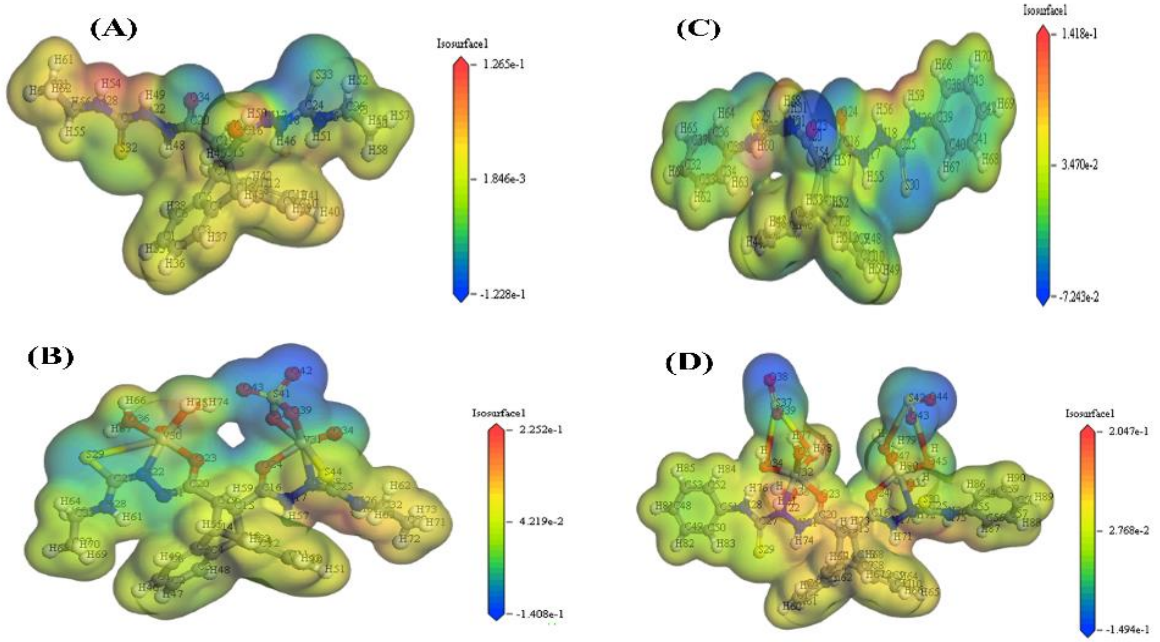

Scheme 5. MEP map for (A)H_4DDET (B); $[(VO)_2(H_4DDET)(H_2O)_2(SO_4)].5H_2O$ (2); (C)H_4DDPT; (D) $[VO)_2(H_4DDPT)(H_2O)_2(SO_4)_2].5H_2O$

Table 5: Kinetic parameters evaluated by Coats-Redfern and Horowitz equations for ligands and their VO^{2+} complexes

Compound	Peak	Mid Temp (K)	Ea KJ\mol	A (S^{-1})	ΔH* KJ\mol	ΔS* KJ\mol.K	ΔG* KJ\mol
H_4DDE	1st	523.57	441.75	6.70×10^{39}	437.4	-0.51282	168.9
		523.86	*450.52*	*5.11×10^{43}*	*446.16*	*-0.5871*	*138.59*
	2nd	530.53	256.04	7.87×10^{20}	251.63	-0.1503	171.87
		529.77	*263.21*	*4.10×10^{24}*	*258.80*	*-0.22150*	*141.46*
$[(VO)_2(H_4DDET)(H_2O)_2(SO_4)].5H_2O$	1st	387.41	13.45	3.37E-01	10.23	-0.2561	109.45
		387.41	*20.35*	*4.31E+00*	*17.13*	*-0.2350*	*108.15*
	2nd	464.35	151.45	1.73E+15	147.59	0.0431	127.57
		464.35	*159.67*	*1.52E+16*	*155.81*	*0.0612*	*127.41*
	3rd	605.25	224.99	4.33E+17	219.95	0.0868	167.40
		605.25	*235.34*	*3.51E+18*	*230.31*	*0.1042*	*167.23*
	4th	695.20	194.04	5.02E+12	188.26	-0.0088	194.38
		695.20	*205.89*	*4.10E+13*	*200.11*	*0.0087*	*194.10*
H_4DDPT	1st	506.35	375.52	$^{34}\times102.12$	371.31	-0.4078	164.81
		507.04	*384.03*	*$^{38}\times101.63$*	*379.82*	*-0.4822*	*135.34*
	2nd	563.74	88.41	$^{3}\times102.02$	83.73	-0.1869	189.11
		565.22	*97.90*	*$^{7}\times101.67$*	*93.20*	*-0.11190*	*156.48*
$[(VO)_2(H_4DDPT)(H_2O)_2(SO_4)_2].5H_2O$	1st	392.94	195.60	21×103.80	192.34	-0.1659	127.14
		392.96	*202.07*	*$^{25}\times102.84$*	*198.80*	*-0.24010*	*104.47*
	2nd	*457.23*	*52.26*	*20×109.24*	48.46	-0.2300	153.61
		456.46	*59.83*	*$^{4}\times107.71$*	*56.04*	*-0.15490*	*126.74*
	3rd	*565.35*	*107.65*	*$^{4}\times105.27$*	*102.95*	*-0.1598*	*193.32*
		585.33	*117.36*	*$^{8}\times104.19$*	*112.49*	*-0.08550*	*162.51*
	4th	847.51	270.71	6.02×10^{11}	263.66	-0.0281	287.47
		846.72	*284.68*	*$^{15}\times104.60$*	*277.64*	*-0.04630*	*238.47*

3.8.3. MEP

The molecular electrostatic potential, MEP which is represents the plot of electrostatic potential mapped onto the constant electron density surface [53]. The 3D plots of MEP (Scheme 4) are drawing whereas the maximum negative region is expressed by red color indicating the available site for the attack by the electrophile. The site for attack by a nucleophile is expressed by a blue cool (i.e., the maximum positive region) [50] and the order; red < green < blue is followed. A glance at the MEP of the investigated hydrazone indicates that N, O and S atoms will have negative potential while H atoms will assign positive potential.

3.9. Biological Studies

3.9.1. Scavenging activities of superoxide radicals

There are two kinds of SOD mimics: metal-dependent and metal-independent mimics. This work focused on the metal dependent SOD mimics, their assays, chemical characters and usage. SOD or the metal complexes catalyze the dismutation of superoxide according to the following equations:

$$Mn^{+n} + O_2^{\cdot} \rightarrow M^{(n-1)} + +O_2 \quad \text{(i)}$$

$$M^{(n-1)} + +O_2^{\cdot} + 2H^{+} \rightarrow Mn^{+n} + H_2O_2 \quad \text{(ii)}$$

$$2O_2^{\cdot} + 2H^{+} \rightarrow H_2O_2 + O_2 \quad \text{(iii)}$$

The present study is used to examine the SOD mimic like activity of the thiosemicarbazides and their VO^{2+} complexes in the PMS/NADH–NBT system. . In this system, superoxide anion derived from dissolved oxygen by PMS/NADH coupling reaction reduces NBT. The decrease of absorbance at 560 nm with antioxidant activities of the complexes indicates the consumption of superoxide anion in the reaction mixture. From the results represented in table 6, it can be concluded that there is an apparent variation in the overall scavenging ability among the parent ligands and their vanadyl complexes. H_4DDPT (3) exhibited the potent activity (82.38%) comparable to ascorbic acid displaying (78.20%) scavenging activities of the superoxide radical followed by H_4DDET (1) (80.47%).The following order of SOD-like activity is observed:H_4DDPT> H_4DDET>$[VO)_2(H_4DDPT)(H_2O)_2(SO_4)_2]5H_2O)$ > $[(VO)_2(H_4DDET)\ (H_2O)_2\ (SO_4)]5H_2O$ which is in good agreement with the literature literature [54] As superoxide is a major factor in radiation damage, inflammation, and tumor promotion. Fortunately, the present study has evolved a defense system against the toxicity of O_2•- by all ligands in general and mono and binuclear VO^{2+}-complexes derived from H_4DDPT in particular.

3.9.2. DNA binding

Examining the DNA degradation assay for all thiosemicarbazides and their VO(II) complexes (fig. 8) revealed variability on their immediate damage on the Calf Thymus (CT) DNA which is used as a positive control. An efficient way to analyze the binding mode and degree of the ligand (HL) and its metal complexes (1–3) with DNA is electronic absorption spectroscopy [55]. The intrinsic constant of binding to CT-DNA was already calculated by tracking the absorption rate of the spectral band of charge transfer for ligands at less or more than 260 nm for the H_4DDET and at 324nm for H_4DDPT and 330 nm of the corresponding binuclear complexes, respectively. The addition of growing quantities of CT-DNA, a significant "hyperchromic" effects have been observed with a mild red change of 2–5 nm in case of H_4DDPT and a more red in case of H_4DDET that is an indicative of DNA helix stabilization. The insertion of a planar aromatic molecule between two adjacent base pairs of DNA is known as intercalation which is stabilized by π–π stacking between the base pairs and aromatic ring system resulting in lengthening, stiffening and unwinding of the DNA helix [55- 57]. This effect however is dependent upon the "depth of insertion". The intercalation is reversible, and is stabilized by a combination of electrostatic, hydrogen bonding, entropic, van der Waals and hydrophobic interactions. The spectral features mean that either the external touch (electrostatic binding) or the major and minor DNA grooves are binding to the ligands and complexes. A glance at figure 8 indicates that, the intrinsic binding constants K_b are in the order of 10^5- 10^7 for all the compounds proving that the compounds under study are strong intercalator when compared with the classical intercalators which are consistent with literature [58]. Therefore, the results can be considered as preliminary experiments and further future biological experiments with different concentrations from each complex will be applied. This allows us to find complexes promising as anti-tumor agent *in vivo* to inhibit the DNA replication in the cancer cells and inhibit the further growth of the tumor.

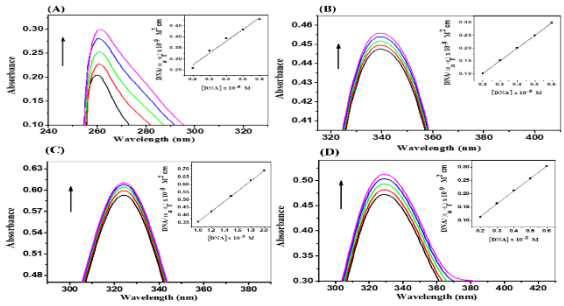

Figure 8. Absorption spectra of (A)H_4DDET (B); $[(VO)_2(H_4DDET)\ (H_2O)_2\ (SO_4)]5H_2O$ (2); (C)H_4DDPT; (D) $[VO)_2(H_4DDPT)(H_2O)_2(SO_4)_2]5H_2O$.

Table 6 ligands and their VO^{2+} complexes on superoxide radicals generated by PMS/NADH system.

Sample	Δ through 5 min	% inhibition
Control	0.450	0.00
L-Ascorbic acid	0.098	78.2
H_4DDET	0.082	80.47
$[(VO)_2(H_4DDET)\ (H_2O)_2\ (SO_4)]5H_2O$	0.289	35.80
H_4DDPT	0.074	82.38%
$[VO)_2(H_4DDPT)(H_2O)_2(SO_4)_2]5H_2O$	0.218	51.5%

Conclusion

Two thiosemicarbazides, H_4DDET and H_4DDPT derivatives form two binuclear complexes with $VOSO_4.H_2O$ salt that were characterized by elemental and spectroscopic techniques. The EPR spectral data confirmed the octahedral geometry for the isolated complexes. The higher values of α^2 and β^2 revealed appreciable covalence in the metal-ligand bonding, presumably arising out of M-thione /thiol coordination. The TG analysis for the title complexes displayed high residual part indicating high stability of the formed chelates. Moreover, all compounds were screened for SOD like activity that revealed potent activity of the thiosemicarbazide derivatives especially H_4DDPT (82.38%) followed by H_4DDET (80.47%) comparable to ascorbic acid. Also, vanadyl complexes exhibited the highest activity among complexes. As superoxide is a major factor in radiation damage, inflammation and tumor promotion, fortunately, the present study has evolved a defense system against the toxicity of O_2 •-by the ligand and its $VO(II)^{2+}$ complexes. The DNA binding assay revealed that the addition of growing quantities of CT-DNA, a significant "hyperchromic" effects have been observed with a mild red change in case of H_4DDPT and a more red in case of H_4DDET that is an indicative of DNA helix stabilization. The insertion of a planar aromatic molecule between two adjacent base pairs of DNA is known as intercalation which is stabilized by π–π stacking between the base pairs and aromatic ring system showed. Further in-depth studies on the mechanism of action of this

mononuclear and binuclear oxovanadium complex would render us with an efficient hypoglycemic drug in the near future.

Acknowledgments
First author gratefully acknowledges the Microbiology Unit at Faculty of Pharmacy, Mansoura University, for carrying out the diabetes experimental work.

References

[1] A.R. Cowley, J.R. Dilworth, P.S. Donnelly, E. Labisbal and A. Sousa: "An unusual dimeric structure of a Cu(I) bis(thiosemicarbazone) complex: implications for the mechanism of hypoxic selectivity of the Cu(II) derivatives", J. Am. Chem. Soc., Vol. 124, (2002), pp. 5270–5275.

[2] C. Q. Debra, A. K. Kathy, R. K. Earl, "New thiosemicarbazone chelates having anticancer activity" Antiviral Res. 71(2006), 24-30.

[3] P Madsen, J M Lundbeck, P Jakobsen, A R Varming, N Westergaard "Glucose-6-phosphatase catalytic enzyme inhibitors: synthesis and in vitro evaluation of novel 4,5,6,7-tetrahydrothieno[3,2-c]- and -[2,3-c] pyridines"Bioorg Med Chem. 8(9)(2000), 2277-89.

[4]T.Varadinova, D.K. Demertzi, M.Rupelieva, M. Demertzis, P.Genova, "ANTIVIRAL ACTIVITY OF PLATINUM (II) AND PALLADIUM (II) COMPLEXES OF PYRIDINE-2-CARBALDEHYDE THIOSEMICARBAZONE"ActaVirol,45 (2001), 45, 87-94.

[5] R.Pingaew, S.Prachayasittikul, S. Ruchirawat, "Synthesis, Cytotoxic and Antimalarial Activities of Benzoyl Thiosemicarbazone Analogs of Isoquinoline and Related Compounds" Molecules, 15 (2)(2010), 988-996.

[6] H Beraldo, D Gambino "The wide pharmacological versatility of semicarbazones, thiosemicarbazones and their metal complexes" Mini Reviews in Medicinal Chemistry, 4(1) (2004),31-39.

[7] N. M. Hosny, Ar.Belal R. Motawea M. A.Hussien and M. H.Abdel-Rhman" Spectral characterization, DFT, docking and cytotoxicity of N-benzyl-4,5-dihydro-3-methyl-5-oxo-1H-pyrazole-4-carbothioamide and its metal complexes" J.Mol Struct.1232 (2021), 130020.

[8] N. M. Hosny, M. A Hussien, R. Motawa, A. Belal, and M. H. Abdel-Rhman" Synthesis, Spectral, Modeling, Docking and Cytotoxicity Studies on 2-(2-aminobenzoyl)-N-ethylhydrazine-1-carbothioamide and its divalent metal complexes" J. App. Organ. Chem.34 (2020),5922.

[9] M. H.Abdel-Rhman, M. A.Hussien, H. M.Mahmoud and N. M.Hosny" Synthesis, characterization, molecular docking and cytotoxicity studies on N-benzyl-2-isonicotinoylhydrazine-1-carbothioamide and its metal complexes" J.Mol Struct. 1196 (2019), 417-428.

[10] O. A. Al-Gammal, A. A. El-Asmy, "Synthesis and Spectral Characterization of 1-(aminoformyl-n-phenylform)-4-ethyl Thiosemicarbazide and its Metal Complexes J. Coord. Chem., 61(14) (2008) 2296-2306.

[11] A. Butler, C.J. Carrano," Coordination chemistry of vanadium in biological systems" Coord. Chem. Rev. 109 (1991), 61-105.

[12] J. M. Arber, E.De Boer, C. D. Garner, S. S. Hasnain, R. Wever," Vanadium K-edge X-ray absorption spectroscopy of bromoperoxidase from Ascophyllum nodosum" Biochem, 28(1989) 7968-73.

[13]T.Hirao,T. Fujii, T. Tanaka, Y.Ohshiro, "A novel regioselective ring-opening oxidation of cyclobutenones with $VO(OEt)Cl_2$"J. Chem. Soc. Perkin Trans. 1(1994), 3-4.

[14] J. Y. Kempf, B. Maigret, D. C. Crans "Four- and Five-Coordinate Oxovanadium(V) Alkoxides: Do Steric Effects or Electronic Properties Dictate the Geometry?" Inorg. Chem.,35(22)(1996), 6485–6494.

[15] D. Skiadopoulos; Diploma Thesis, Diabetes mellitus, Charles University in Prague, Faculty of Pharmacy in Hradec Kralove, Department of Biological and Medical Sciences, 2013.

[16] P. Go´mez-Saiz, J. Garcı´a-Tojal, M.A. Maestro, F.J. Arnaiz, T. Rojo," Synthesis, X-ray characterization, DFT calculations and Hirshfeld surface analysis of M n+ ions (n = 2,3; M = Ni, Cd, Mn, Co and Cu): The role of secondary bonding and steric effects in complexes based on thiosemicarbazone" Inorg. Chem. 41 (2002) 1345.

[17] G. Canil, S. Braccini, T. Marzo, L. Marchetti, A. Pratesi, T.Biver, T.Funaioli, F. Chiellini, J. D. Hoescheled, C. Gabbiani "Photocytotoxic Pt(iv) complexes as prospetive anticancer agents" Dalton Trans.,(2019), 48, 10933–10944.

[18] C. R. Kowola, N. V. Nagy, T. Jakuschd, A. Rollera, P. Heffeter, B. K. Kepplera, É. A. Enyedyd; "Oxovanadium(IV) complexes of bromo and methoxy substituted N1 ,N4-diarylidene-S-methylthiosemicarbazones "Cent. Eur. J. Chem.; 4(1) 2006 149–159.

[19] L.S. Chin, S.F. Murray, D.H. Harter, P.F. Doherty and S.K. Singh: "Sodium vanadate inhibits apoptosis in malignant glioma cells: a role for Akt/PKB", J. Biomed. Sci., Vol. 6, (1999), pp. 213–220.

[20] M.R. Maurya, S.K. Shailendra, A. Azam, W. Zhang and D. Rehder: "Biological and medicinal aspects of vanadium", Eur. J. Inorg. Chem., Vol. 24, (2003), pp. 4397– 4402.

[21] M.T. Pope and A. Muller (Eds.): ¨ Polyoxometalates: From Platonic Solids to AntiRetroviral Activity, Kluwer Academic Publishers, Dordrecht, 1994.

[22] P.J. Stankiewicz, A.S. Tracey, D.C. Crans, H. Sigel and A. Sigel (Eds.): Vanadium and its Role in Life, Metal Ions in Biological Systems, vanadyl 31, Marcel Dekker, New York, 1995.

[23] A.K. Srivastava: "Anti-diabetic and toxic effects of vanadium compounds", Mol. Cell. Biochem., 206, (2000), 177–184.

[24] D.C. Crans: "Chemistry and insulin-like properties of vanadium(IV) and vanadium(V) compounds", J. Inorg. Biochem. 80 (2000), 123–129.

[25] R. G. Bhirud, S. Srivastava"Synthesis, characterization and superoxide dismutase activity of some ternary copper(I1) dipeptide-2,2'-bipyridine, l, l0-phenanthroline and 2,9-dimethyl-l,lO-phenanthroline complexes" Inorg.Chim Acta, 179 (1991) 125-131.

[26]A. L.Abuhijleh, J. Khalaf "Copper (II) complexes of the anti-inflammatory drug naproxen and 3-yridylmethanol as auxiliary ligand. Characterization, superoxide dismutase and catecholase – Mimetic activities" Eur. J. Med.l Chem. (2010), 45(9):3811-7.

[27]A.L.Abuhijleh "Mononuclear copper (II) salicylate complexes with 1,2-dimethylimidazole and 2-methylimidazole: Synthesis, spectroscopic and crystal structurecharacterization and their superoxide scavenging activities", J. Mol. Struct980, (2010)201–207.

[28] E. T. Pirc,B.Modec, K. Cer-Kercˇmar, P. Bukovec" Synthesis, structure, antioxidant and SOD-mimetic activity of [Cu(xanthurenate)(nicotinamide)(H_2O)] complexes" Monatsh Chem 145(2014), 911–920.

[29] G. Jeffery, J. Bassett, J. Mendham, R. Denney, Vogel's quantitative chemical analysis, 5 th ed., Longman Scientific & Technical Longman Group UK Limited, Essex CM20 2JE, England, 1989.

[30] O.A. El- Gammal, I.M. Abd Al-Gader , A.A. El-Asmy" Synthesis, characterization, biological activity of binuclear Co(II), Cu(II) and mononuclear Ni(II) complexes of bulkymulti-dentate thiosemicarbazide" Spectrochim. Acta Part A:128(2014) 759–772.

[31] M. R. Mlahi , O.A. El-Gammal, M. H. Abdel-Rhman" Synthesis, characterization, DFT molecular modeling and biological studies of Zn(II), Cd(II) and Hg(II) complexes of new polydentate thiosemicarbazide" J.Mol. Struct; 1182 (2019) 168-180.

[32] O.A El-Gammal, M Gaber, SA Mandour "Novel VO (IV) complexes derived from a macrochelates: Synthesis, characterization, molecular modeling and in vivo insulin-mimic activity studies" Journal of Appled Organometallic Chemistry; 34 (9) (2020), 5699.

[33] A. M Zaghloul, A. A Gohar, Z. Al-abdin M Naiem, F.M Abdel Bar" Taxodione, a DNA-binding compound from Taxodium distichum L. (Rich.); Z Naturforsch C J Biosci. 63(2008);5-6.

[34] Ola A. El-Gammal, Farid Sh. Mohamed, Ghada N. Rezk, Ashraf A. El-Bindary"Structural characterization and biological activity of a new metal complexes based of Schiff base" Journal of Molecular Liquids,330(2021) 115522.

[35] An ab initio molecular orbital study of the conformational energies of 2-alkyltetrahydro-2H-pyrans (tetrahydropyrans, oxacyclohexanes, oxanes) J. Mol. Structure: THEOCHEM; 496, Issues 1–3,(2000) 19-39.

[36] A. Kessi, B. Delley, "Density functional crystal vs. cluster models as applied to zeolites"Int. J. Quantum Chem. 68(1998) 135.

[37] B. Hammer, L. B. Hansen, J. K. Nørskov "Condens. Matter, "Improved adsorption energetics within density-functional theory using revised Perdew-Burke-Ernzerhof functionals", Phys. Rev. B 59 (1999) 7413-7421.

[38] O.A. El-Gammal, G.M. Abu El-Reash,R.A. Bedier" Synthesis, spectroscopic, DFT, biological studies and molecular docking of oxovanadium (IV), copper (II) and iron (III) complexes of a new hydrazone derived from heterocyclic hydrazide":App. Organ.Chem., (2019), 5141, pp1-14.

[39] O. A. El- Gammal, G. M. Abu El-Reash, , M. M. El-Gamil," Structural, Spectral, pH- metric and biological studies on mercury(II), cadmium(II) and binuclear zinc (II) complexes of NS donor thiosemicarbazide ligand" Spectrochim.Acta Part A (2014):59 – 70.

[40] A.A. El-Asmy, O. A. Al-Gammal and H. Saleh,"Synthesis, Spectral Characterization and Analytical Application of Cd(II) and Hg(II) complexes of Some Thiosemicarbazones Spectrochimica Acta,

[41] K. Nakamoto, Infrared and Raman of Inorganic and Coordination Compounds, 2nd ed., Wiley, New York, 1970.

[42] M. H.Abdel-Rhman, R. Motawea, A. Belal, and N. M.Hosny" Spectral, structural and cytotoxicity studies on the newly synthesized n'[1],n'[3]-diisonicotinoylmalonohydrazide and some of its bivalent metal complexes" J. Mol. Struct.1251(2022), 131960.

[43] N M. Hosny, N Y. Hassan, H M. Mahmoud, and M H. Abdel-Rhman "Synthesis, characterization and cytotoxicity of new 2-isonicotinoyl-N-phenylhydrazine-1-carbothioamide and its metal complexes" J. Appl. Organ. Chem. 33(2019)4998.

[44] N M.Hosny, N Hassan, H M.Mahmoud, and M H.Abdel-Rhman" Spectral, optical and cytotoxicity studies on 2-isonicotinoyl-N-phenylhydrazine-1-carboxamide(H3L) and some of its metal complexes" J of Mol Struct 2018.1156.602-611.

[45] O.A. El-Gammal, I.M. Abd Al-Gader, A.A. El-Asmy;" Synthesis, characterization, biological activity of binuclear Co(II), Cu(II) and mononuclear Ni(II) complexes of bulky multi-dentate thiosemicarbazide" Spectrochimica Acta Part A:128, (2014)759–772.

[46] S. Kuwajima , Y. Arai, H. Kitajima , Y. Kikukawa, Y. Hayashi ," Synthesis and structural characterization of tube-type tetra-decavanadates" Acta Crystallogr C Struct Chem. 2018 Nov 1;74(Pt 11):1295-1299.

[47] Y.-R. Gong, W.-C. Chen, L. Zhao, K.-Z. Shao, X.-L. Wang, Z.-M. Su, Functionalized polyoxometalate-based metal–organic cuboctahedra for selective adsorption toward cationic dyes in aqueous solution, Dalton Transactions, 47 (2018) 12979-12983.

[48] O.A. El-Gammal and M.M. Mostafa" "Synthesis, characterization and molecular modeling of Girard′Tthiosemicarbazide and its complexes with some transition metal ions" Spectrochim. Acta. Part A: (2014) 530-542.

[49] O. A. El-Gammal, F.E.El-Morsy, B.Jeragh, A. A. El-Asmy.,."Chelation Behavior of bis(1-(pyridine-2-yl) ethylidene)-Malonohydrazide towards some Transition metal Ions" Canad.Chem. Trans. 1(4) (2013) 277-291.

[50] A.Broido, "A simple, sensitive graphical method of treating thermogravimetric analysis data" J. Polymer Sci., 7 (1969) 1761-1773.

[51]O.A.El-Gammal,"Synthesis, Characterization and Antimicrobial Activity of 2-(2-ethylcarbamothioyl)hydrazinyl) -2-oxo-N-phenylacetamide copper complexes Spectrochim. Acta Part A, 75, 533(2010).

[52] O. A. El-Gammal, T. H. Rakha, H. M. Metwally, G. M. Abu El-Reash, "Synthesis, characterization, DFT and biological studies of isatinpicolinohydrazone and its Zn (II), Cd (II) and Hg (II) complexes", Spectrochim. Acta. A, 127, (2014) 144-156.

[53] Ola A. El-Gammal, Farid Sh. Mohamed, Ghada N. Rezk, Ashraf A. El-Bindary" Structural characterization and biological activity of a new metal complexes based of Schiff base" J. Mol. Liq.; S0167-7322(21)00248-8 (2021).

[54] O.A El-Gammal, M Gaber, SA Mandour "Novel VO (IV) complexes derived from a macrochelates: Synthesis, characterization, molecular modeling and in vivo insulin-mimic activity studies" Journal of Appled Organometallic Chemistry; 34 (9), 5699 (2020).

[55] Ola A. El-Gammal, Farid Sh. Mohamed, Ghada N.Rezk, Ashraf A. El-Bindary. ."Synthesis, characterization, catalytic, DNA binding and antibacterial activities of Co(II), Ni(II) and Cu(II) complexes with new Schiff base ligand "J. Mol. Liq.; 326, 11522 (2021).

[56] H.A. Kiwaan, A.S. El-Mowafy, A.A. El-Bindary, Synthesis, spectral characterization, DNA binding, catalytic and in vitro cytotoxicity of some metal complexes, J. Mol. Liq. 326 (2021) 115381

[57]M. E. Özgür · A. Ulu · C. Gürses· İ. Özcan · S. A. A. Noma · S. Köytepe · B. Ateş; "Structural characterization and DNA binding properties of a new imine compound" Biological Trace Element Research (2022).

[58] C. Gürses , A. Aktas¸ S.i Balcıoglu, A. Fadhilahe, Y. Gökc, B.Ates" Synthesis, characterization, DNA binding and anticancer activities of the imidazolidine-functionalized (NHC)Ru(II) complexes" J.Mol. Struct. 1247, (2022), 131350.